Int. J. Bio-Inorg. Hybr. Nanomater., 8(1): 27-37, Spring 2019

Novel application of hybrid Perovskite materials in grid-connected photo-voltaic cells

P. Alemi*

Department of Electrical Engineering, Urmia branch, Islamic Azad University, Urmia, Iran

Received: 27 October 2018; Accepted: 30 December 2018

ABSTRACT: In this paper, the novel application of organic/inorganic perovskite hybrid materials is proposed for grid-connected Photo-voltaic (PV) cells. The perovskite hybrid cells attracted a lot of interest due to their potential in combining advantages of both components. Looking to the future, there is no doubt that these new generations of hybrid materials, born from the very fruitful activities in this research field, will open a land of promising applications in many areas such as solar cells and fuel. In other view due to world energy requirements, the integration of solar energy will diminish the consumption rate of non- renewable energies and also dependency of fuel cells. The PV cells are utilized the sun energy and generate the DC power where the converters are utilized for boosting the low output voltage of PV cells and converting the DC to AC grid voltage respectively. The Maximum Power Point Tracking (MPPT) method based on Perturb and Observe (P & O) algorithm is used to operate the PV cell in point of maximum power. The three-phase current source inverter (CSI) as a DC/AC converter is utilized for grid connection of PV. The simulation by MATLAB/SIMULINK is done to show the effectiveness of the proposed method.

Keywords: *Converter, Grid, MPPT, Perovskite hybrid materials, PV.*

INTRODUCTION

In recent years, the rapid increasing of world energy consumption is become an important issue, and 20% more gain in growing of energy utilization is predicted by 2040 [1-3]. Due to the effects in emissions of green-house gas, acid rain, and air pollutions, the growth of renewable energy, including wind, water, and solar energies, has become a crucial concern. By a simple checking in renewable energy resources, the solar energy is promising candidate. The life expectancy, low maintenance costs and statics are the main advantages of PV systems. Extracting the maximum power from the PV array is a big issue in which various MPPT methods are introduced [4-7]. The various types of PV cells have been developed and tested and among the numbers of techniques, the photon to electricity conversion has been attempted over the years and the use of semiconducting materials has been the most successful. The PV materials such as inorganic semiconductor nanoparticles, silicon, organic dyes, conducting polymers, and also combinations have already been attempted. In the last decades hybrid materials were expanded a lot by realizing economic applications. Multi-

(*) Corresponding Author - e-mail: payamalemi@gmail.com

ple-functional materials can be made by designing the properties of hybridization in organic and inorganic materials [5], [8-10]. Although the silicon PVs like crystalline-Si (c-Si) dominate more than 90% of solar panel market, the novel emerged photovoltaic technologies like dye sensitized solar cells (DSSCs) which will be evaluated by oxides and mixed oxides semiconductors, organic solar cells (OSCs), and perovskite solar cells (PeSCs) have gained more attention due their good properties, such as low-cost, light weight, low fabrication temperatures, and mechanical flexibility. There is no doubt that, every type of these new materials has their advantages/disadvantages. The optimizations in component structures, conditions of deposition, and composite manipulation are the factors which made the progress in PeSC efficiencies [11-15]. The power conversion efficiencies (PCEs) of certificated PCEs of DSSCs, OSCs, and PeSCs are about 11.9%, 11.5%, and 23.3%, respectively, according to the recent report from the National Renewable Energy Laboratory (NREL). The PCEs of new topologies cannot reach conventional types, however these technologies displaying unique properties and there is no doubt for their utilization in near further [12–14]. Due to increasing interest in grid connected PV systems, the operation of PV application which utilized new hybrid materials are gained a lot of attention. The advantages of novel materials like lower weight could be an important issue in connecting several PV modules in series and parallel to have the appropriate DC voltage levels and enough power to the central inverter in lower cost. The AC/DC converter in series with DC/DC boost converter is utilized for PV cells connection to grid in which the DC/DC converter match the level of the grid voltage without the need for an additional conversion stage [16]- [18].

In this paper, the application of hybrid perovskite materials in grid- connected photo-voltaic cells is presented. In section II, the Organic/Inorganic, and hybrid materials in PV cells are described and the nonlinear characteristic and electrical model of PV is presented in section III. The structure of grid/load connected system is presented in section IV. In section V, the simulation results are investigated and finally conclusion is presented.

The organic/inorganic and hybrid materials in PV cells

Organic and inorganic materials

The properties of inorganic materials such as metals, ceramics and organic compounds like polymers could be investigated by their applications. Table 1, listed some of general properties of conventional organic/inorganic materials. In case of organic conducting polymers, the different chemical structures such as possessing promising properties, like simple process-

Table 1. The properties of conventional organic and inorganic components

Properties	Organics (polymers)	Inorganics (SiO_2, TMO)
The nature of bonds	covalent [C – C] (+ weaker van der waals or H bonding)	ionic or iono-covalent
Tg (glass transition)	Low-2100 uC to 200 uC	High-200 uC
Thermal stability	Low-350 uC, except polyimides, 450 uC	High-100 uC
Density	0.9 to 1.2	2.0 to 4.0
Refractive index	1.2 to 1.6	1.15 to 2.7
Mechanical properties	elasticity plasticity rubbery (depend on Tg)	hardness strength fragility
Electronic properties	insulating for conductive redox properties	insulating to semiconductors (SiO_2, TMO) redox properties(TMO) magnetic properties

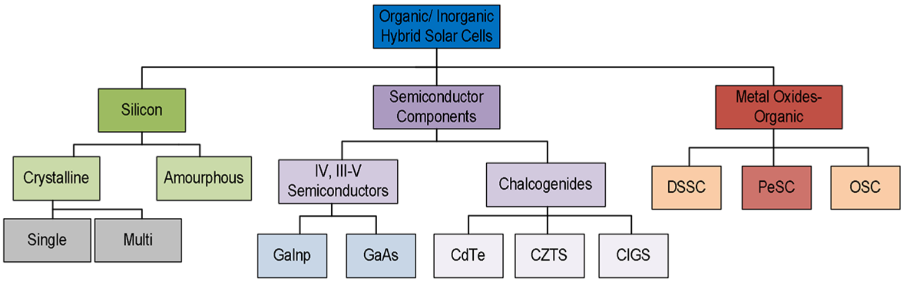

Fig. 1. The classification of hybrid solar cells.

ing, possible recyclability, comparatively lower cost, similar applicability and scalability like sustainable materials are obtained. In the other side for inorganic semiconductors, having preferable electronic properties, as an example a high dielectric constant, and thermal stability, photo-conducting and luminescent properties. To have the advantage of both organic/inorganic materials, hybrid nano composites of inorganic semiconductors and conducting polymers are of great interest, particularly as candidates for the materials of PV cell, in which the composed absorption band of both materials could harvest sun light in better manner [2-5].

Hybrid materials

Until now, many studies are performed to find the good composition of inorganic/organic components and optimum hybrid architectures have been proposed. However, the PCE still has not caught up to the good level and we believe there is room to improve the hybrid organic/inorganic photovoltaic materials. The hybrid materials can show better properties in compare with other materials. The inorganic materials can perform multiple roles such as increasing mechanic and thermic stability, preparing available poriferous network for sensing, or contributing special magnetic, electric, electro-chemical or chemical properties. The organic materials greatly expand range of matrices accessible for synthetic chemists. These materials can propose some chances for modifying the mechanical properties providing manufacturing of films and fibers, to get different geometric structures by simple casting for unified optics, for controlling networks porosity and connectivity, and for adjusting the balance hydrophilic/hydrophobic character. The advantage of hybrid PVs in compare with organics are their higher carrier mobility and less absorbing in longer wave-lengths. On the other side, the existed organic materials in hybrid solar cells, made the superior performance versus conventional semiconducting PVs in view of cost, efficiency, lightweight, and malleability. In addition, the development of new semiconducting nanostructures in composition by organic nano-materials as an example fullerenes and carbon nanotubes (CNTs) opens novel chances to prevail 10% barrier of conversion efficiency for hybrid solar cells in near future.

The different types of hybrid PVs depending on utilized organic and inorganic materials and the morphology of devices are illustrated in Fig. 1. The hybrid solar cells based on Group IV (Si) and Group III-V (mostly GaAs) semiconductors forming the hetero-junction by different organic components are shown in middle column and for general purposes, other types of hybrid PVs are also described. The DSSCs [9, 11] is perhaps the most well checked hybrid solar cells which is combined of nanoporous metal oxide (usually TiO_2) infiltrated by sensitized dye molecules (ruthenium based “N3” dye) and liquid electrolyte. The next class of hybrid PVs as shown in Fig. 1 is identical to DSSC due to the similar nanoporous metal-oxide inorganic matrixes as an example for TiO_2 and ZnO_2 combined in architecture of device. The perovskite component is also embedded between mesoporous TiO_2 layer, which is permeated by the perovskite, and a high-work-function hole-transporting layer (HTL). The PeSCs not only exhibit very high PCEs under normal sun illumination conditions but also behave outstandingly under dim-light illumination [7-12].

Nonlinear specification and the electrical model of hybrid PV cells

There are different equivalent circuit model for the

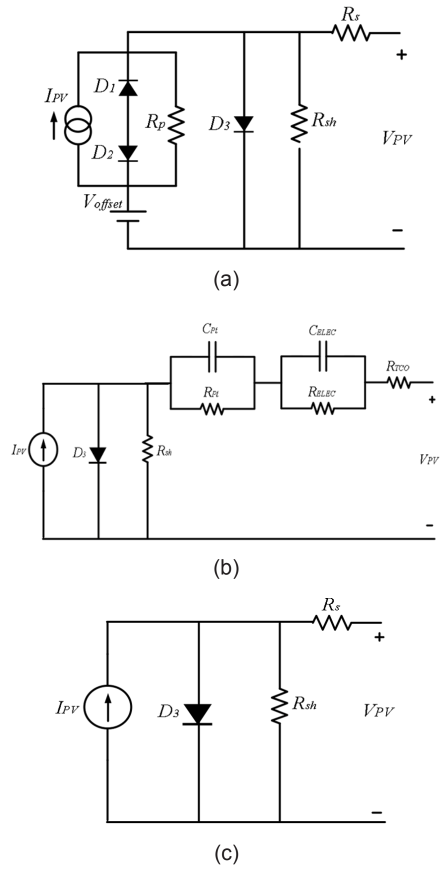

Fig. 2. The equivalent circuit of solar cells. (a) Organic PV cells. (b) DSSC PV cells. (c) Perovskite PV cells.

organic, DSSC and perovskite solar cell which are mathematically modelled based on electrical characteristics and illustrated in Fig. 2. The equivalent circuit model of perovskite PV cell is illustrated in Fig. 1c. This model is the most popular model to represent a PV module. The current source as a PV photo current (Ipv) is employed in parallel with a diode, with parallel and series resistor where the system output is directly affected by solar irradiance and temperature [2]. The list for PV cell circuitry elements and their physical effects are listed in Table 2. The surface recombination and trapping effects are mostly provided in photocurrent generating process. The series resistance (RS) presents ohmic dropping of voltage at contacts and through the layers of various materials. So RS value can change under diverse illuminations and types of cells. The RS decrease the short-circuit current but it has no effect on open circuit voltage. The RS parameter becomes more important when the irradiance and cell temperatures values are more different than their reference value [5-7]. The shunt resistance (RSh) is theoretically very high which is due to the reverse saturation current of the active junction. In real solar cells there are some partial shorts of the junctions due to the formation of pinholes and metal filling of these pinholes reaching to the junction. There is no effect of RSh on short-circuit current, but it diminish the open-circuit voltage. The effect of RS and RSh on the I-V graph of perovskite PV cell is illustrated in Fig. 3 and Fig. 4 respectively. There are several methods for finding the appropriate value for RS which shows the effect of the internal resistance and the contacts of the cell. It is more convenient to write the electrical equation of PC cell as:

$$I = I'_S - I_o\left(e^{q(V+IR_s)/\mu_0 kT} - 1\right) - \frac{V+IR_s}{R_{sh}} \qquad (1)$$

where,

I'_s: Short-circuit current when there are no parasitic

Table 2. The circuit elements, their effects, and applications

Circuit Element	Effect	Application
Current source	The excitation of electron by photons	All cells
Ideal diode	Current diffusion from base and emmiter	All cells
Series resistor	The resiatance of layer and contacts	MPPT, Power loss analysis
Parallel resistor	Modelling of recombinaion	Fault diagnosis analysis
Capacitors	Cell-layers capacitances	Dye sensitized cells
Double diode	Generation of junction space-charge region	Polycrystalline cells
Avalanche current source	Reverse bias in shading	Partial shading condition (PSC)
Embedded in photocurrent	Surface recombination and carrier trapping	All cells

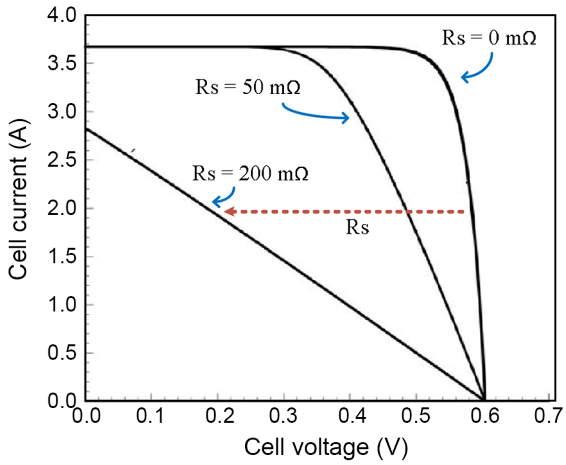

Fig. 3. The effect of series resistance on the perovskite cell I-V graph by assuming Rsh size is infinite.

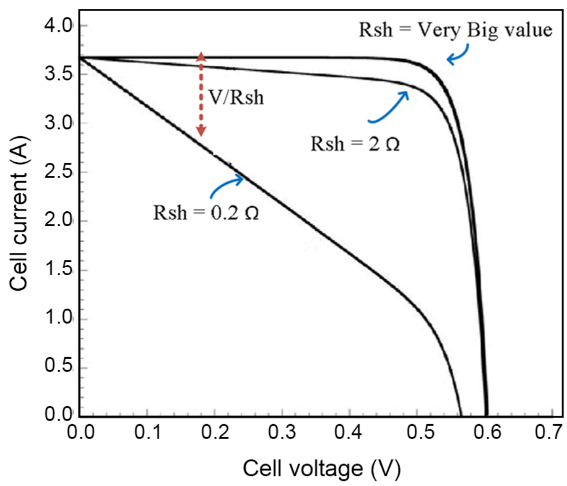

Fig. 4 . The effect of shunt resistance on the perovskite cell I-V graph by assuming Rs size is zero.

resistances,

I_0: Reverse saturation current,

k: Boltzmann's constant (1.381×10^{-23} J/K),

T: Kelvin temperature

q: Unit charge

In short circuit condition, (1) becomes,

$$I = I_S' - I_o\left(e^{qI_{SC}R_S/\mu_0 kT} - 1\right) - I_{SC}\frac{R_S}{R_{sh}} \tag{2}$$

And by considering open circuit condition, due to have zero I'_s, the open circuit voltage (V_{oc}) could be write by,

$$0 = I_{SC}' - I_o\left(e^{V_{OC}/\mu_0 kT} - 1\right) - V_{OC}/R_{sh} \tag{3}$$

By combining (2) and (3),

$$I_{SC}R_s = \frac{\mu_0 kT}{q} Ln\left(e^{V_{OC}/\mu_0 kT} - I_{SC}/I_0\right) \tag{4}$$

$$V_{OC}/R_{sh} = I_{SC} - I_0 e^{qV_{OC}/\mu_0 kT} \tag{5}$$

where the plot of I_{sc} versus $\log(I_0 e^{qV\infty/\mu 0kT} - I_{sc})$ will utilize to extract the R_s in (4) and R_{sh} can be determined by the slope of line given by plotting V_{oc} versus $I_{sc} - I_0 e^{qV\infty/\mu 0kT}$.

The cell V_{oc} is given by related equation based on perovskite PV cell energy band gap as:

$$V_{OC} = \frac{E_g}{q} - \frac{nKT}{q} Ln\left(\frac{I_{0\,max}}{I_{SC}}\right) \tag{6}$$

where,

Eg : band-gap energy,

n : the electron density,

I_{omax}: maximum reverse saturation current.

The band gap (Eg) of the perovskite material can be continuously tuned from around 1.6 to 2.3 eV. Also if Sn compositions are included, it can be decreased down to ~1.2 eV. This particular aspect of perovskites makes them especially attractive for multifunction or tandem solar cells. For a good solar, the series and shunt resistances should be very small and large respectively [10-12]. For commercial solar cells, the parallel resistance is much bigger than the forward resistance of a diode. As a design example, the perovskite material with Eg equal 1.56 ev is selected for PV cell and by utilizing 4-6, the parameter values are calculated which are listed in Table 3.

Structure of the Grid/Load connected PV system

In this section the structure of grid/load connected PV systems is explained in which the PV cell is utilized a DC/DC boost converter plus DC/AC converter to generate the appropriate AC voltage level for grid connection. Fig. 5 illustrates the block diagram of the proposed system. It includes a MPPT method to operate the PV cell in its maximum power point and next the DC/DC boost converter is used to boost the PV

Table 3. The calculated values of perovskite PV cell.

	Eg	V_{oc}	R_s	R_{sh}	I_{sc}
PV cell	1.56 eV	0.86	9	773	16.9

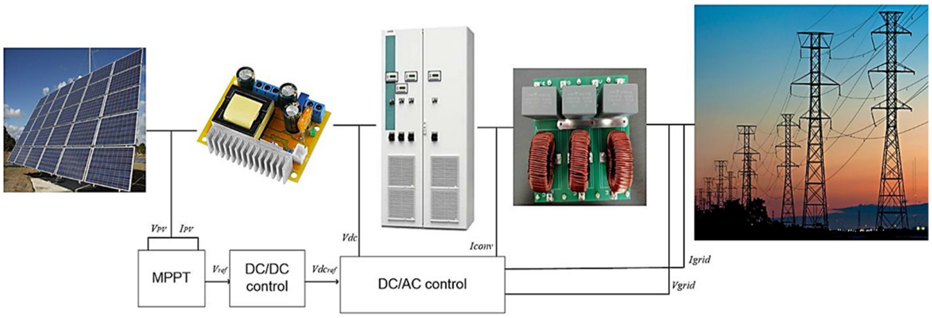

Fig. 5. The block diagram of proposed grid-connected PV cells

output voltage to the appropriate DC voltage level to connect DC/AC power converter. Finally the DC/AC converter is utilized to convert the DC to AC which could be connected to grid or load. Each converter has the control algorithms, considering the role of preparing maximum power to the grid or loads. The first converter is a boost DC/DC that is used to track the maximum electrical energy generated by the PV array, for various irradiance and temperature values, utilizing basic MPPT algorithm type Perturb and Observe (P&O) [19-22]. The second converter is a three-phase current source converter inverter (CSI) which is connected to the AC side by means of LC filter. The LC filter is placed in AC side and having the role of suppressing the PWM harmonic distortion and providing good stability in terms of amplitude and frequency in various values of resistive loads or grid currents. Therefore there are three main sections of PV connection to AC load or grid. (a) PV array and utilized P&O MPPT algorithm, (b) DC/DC Boost converter, (c) Three-phase CSI DC/AC converter.

PV Array and P&O MPPT Algorithm

Due to low output rated power of the perovskite PV cells which is varies between 1 and 2 W and the grid requirements in generating higher voltage and current levels, the designers are encouraged to utilize series and parallel connections of PV cells to ensure the desired level of output voltage and power by PV array [3]. Therefore utilizing photovoltaic panels which uses the several parallel and series connections of PV cells is the appropriate way in every kind of PV cells, every perovskite PV array is constructed by series and parallel connections of many PV cells. The series connection of modules named string. It is clear that, the number of modules and PV cells inside of them are important in determining the PV peak current. Also there will be some problems like hot-spot in which the protections of module against hot-spot can be done by utilizing bypass diodes in parallel connection with each module and the possibility of potential difference phenomena between series connected strings is solved by adding a blocking diode in series with each string. The PV array configuration is illustrated in Fig. 6a where several PV cells are connected in series and parallel. In addition, higher power levels installations

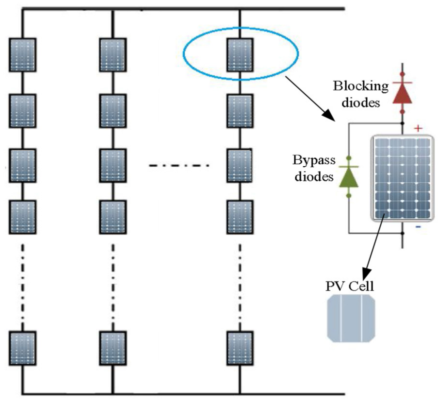

(a)

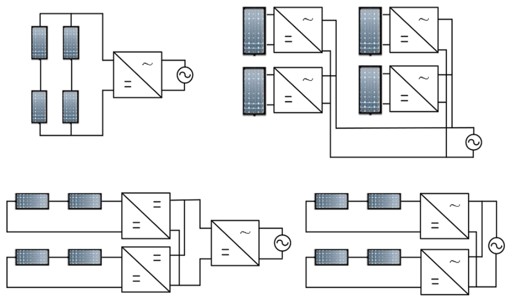

(b)

Fig. 6. The PV array. (a) configuration. (b) The various panels connections.

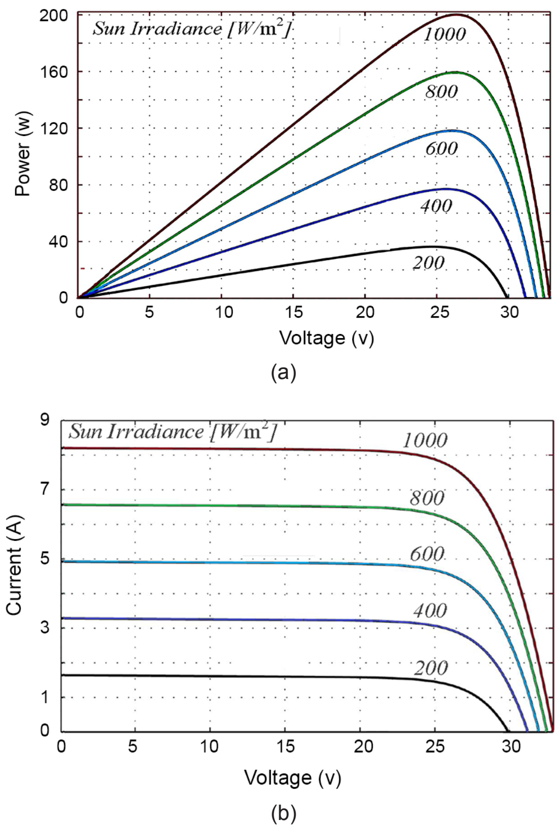

Fig. 7. The perovskite solar cells characteristics by different values of sun irradiance in the fixed temperature (T = 25 °C). (a) P-V graph. (b) I-V graph.

could be made by series and parallel connections of panels. So it is mandatory to have series and parallel connections of panels in various configurations which are identified for PV arrays and inverters to generate a power for grid connection in Fig. 6b. The current versus voltage (I-V) and power versus voltage (P-V) curves associated with the specific PV array is utilized in various values of solar irradiance and fixed temperature (Fig. 7).

It is clear that, even though the PV array is produced various power values in each specific atmospheric status depending on the solar irradiance level and temperature, there is only one point of power that is considered as the maximum power point (MPP). There is one MPP for each curve, considering the shading is negligible and in case there will be a shading effect, the partial shading MPPT methods are proposed [18-19]. The PV array should generate the maximum power by utilizing the specific approach to track this maximum power which is generally named maximum

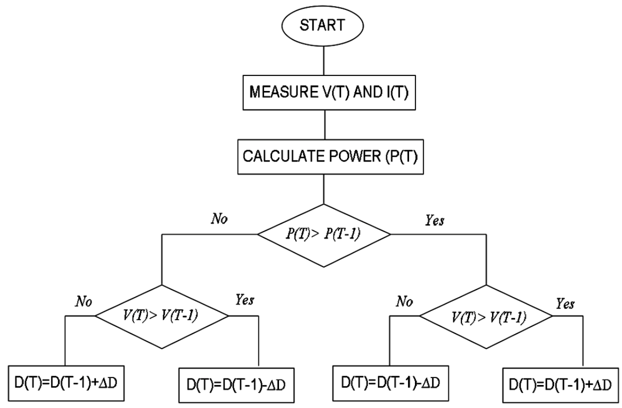

Fig. 8. The P&O MPPT algorithm.

power point tracking (MPPT) method. In this work, the P&O MPPT algorithm is applied for PV array voltage, in which a little perturbation is stated and perturbation causes the solar module power to alter in continues condition. This MPPT algorithm is illustrated in Fig. 8 where in case of power enhancing because of perturbation, the perturbation is continued in similar direction. The power at next instant diminished after reaching the peak power, and after that perturbation is reversed. By reaching the steady-state condition, the algorithm oscillates around peak spot. The size of perturbation is kept very small to have low power variation [18].

DC/DC Boost converter

In the presented PV system, the second block after PV array is a DC/DC boost converter (Fig. 9) for stepping up the PV array output voltage to have appropriate condition for input DC voltage of AC/DC converter and also catching MPP in various atmospheric conditions. The DC/DC boost converter is a class of switched-mode power supply (SMPS) comprising two semiconductors (a diode and a transistor) and one energy storage element such as capacitor, inductor, or the composition at least. For voltage ripple reduction, the capacitor filter or its combination with inductor is added to converter's output- and input-side.

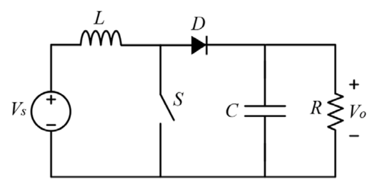

Fig. 9. The DC/DC Boost converter.

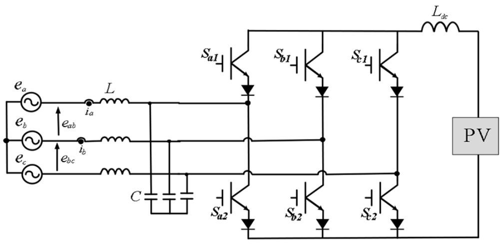

Fig. 10. Three-phase CSI grid connected PV.

Three-phase CSI converter

The Three-phase grid-connected CSI with the proposed control algorithm is illustrated in Fig. 10. By using IGBTs in CSI structure, the reverse blocking capability can be obtained by utilizing series diodes which yields relatively high semiconductor conduction power losses. Another alternative is the reverse blocking IGBT (RB-IGBT). The proposed MPPT algorithm which is used to operate the PV in MPPT point, provide the reference DC voltage for DC voltage controller. The output of voltage controller provide the current reference and the AC-side current controllers are designed in the *dq*-reference frame and responsible to generate the voltage reference in *dq*-reference frame. The converter operated by SVPWM method which is responsible to generate the gating signals of CSI by utilizing the generated reference voltage by current controllers. To suppress the PWM switching harmonics of CSI, the LC filter before connecting the grid and the DC filter inductor in DC-side of converter is provided. The filter parameters are designed based on the designed rule in the switching frequency of converter [22-26].

Simulation results

To evaluate the performance of the proposed method, the simulation has been carried out for the grid- connected PV system under the condition listed in Table

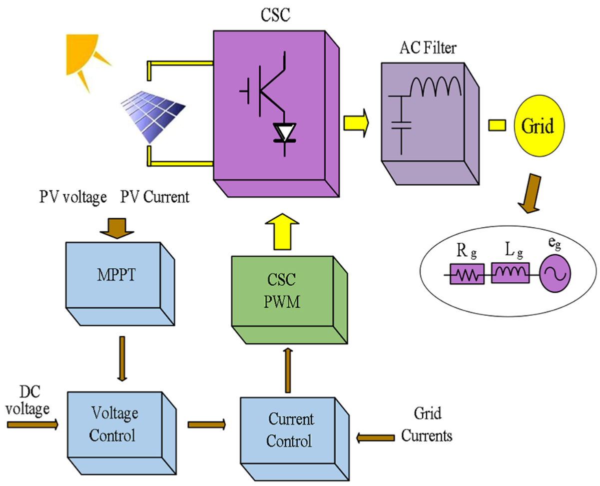

Fig. 11. PV System Control block diagram.

4. The 1 MW power range is decided to operate CSI and the 600V, 1600A RB-IGBT devices are used in selected topology. By considering the 1000V DC- voltage, the input AC voltage of CSI could be set to 816 V_{rms} where we don't need to have a lower AC lines in compare with VSI and the PWM switching frequency is designed in 3 KHz which could meed the design requirements.

The filter parameters have been designed based on the procedure for AC- and DC- filter design. By performing the designed MPPT method and finding the reference DC voltage as 1000V the voltage control has been done and the converter q-axis current reference is produced as output of DC-voltage control. The q-and –d axis current control is done by PI current controllers for CSI operation. The system control block diagram is illustrated in Fig. 11, where the output of proposed MPPT is used for controlling the DC voltage by which the output of voltage controller is used as an input of current controller. The outputs of current controllers are used for generating the gaiting signals in CSI. The simulation results for PV system in

Table 4. Simulation parameters for CSI and filter

Parameters of PWM Inverter		Filter Parameters	
Power rating	1 MW	Output AC filter	L 0.057 p.u
Input AC voltage	816 V_{rms}/50 Hz		C 0.062 p.u
DC-link voltage	1000 V	Input DC inductor	0.038 p.u
Switching frequency	3 kHz	DC-link capacitance	0.02 u

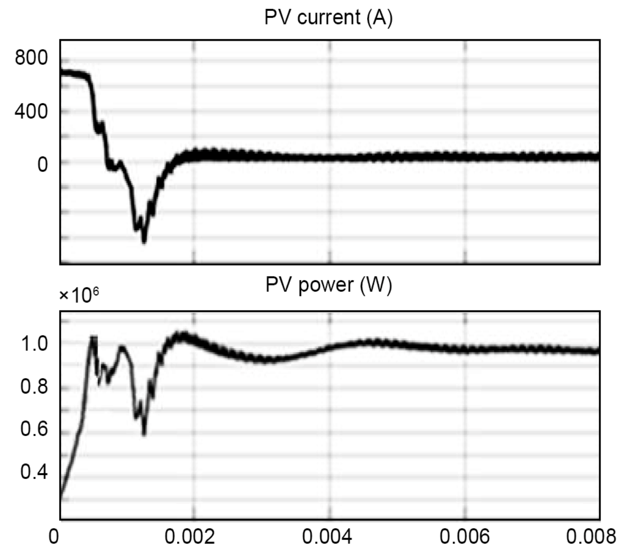

Fig. 12. Simulation results for PV system under PSC in case GMPP is in first point.

case maximum power point is in the beginning points of graph are illustrated in Fig. 12 where the presented MPPT algorithm could detect the MPP.

In Fig. 13, the PV operation is illustrated. By detecting the maximum power, the q-axis current is assumed as an active component and decreases by reducing the irradiance level to half and the d-axis current is kept at zero for achieving unity power factor operation. It is seen that the grid current follows well its reference when the current reference is changed. It is known by PV curve that, the dc voltage variation which is just about 20 V is much lower than the current changes

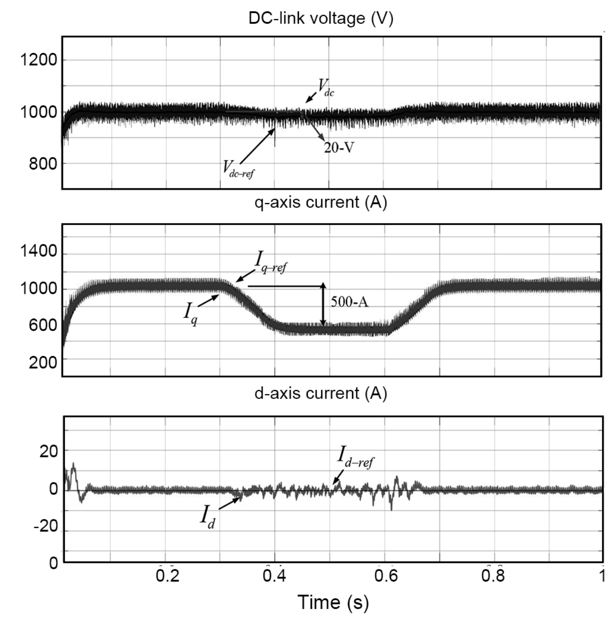

Fig. 13. Simulation results for controller performance.

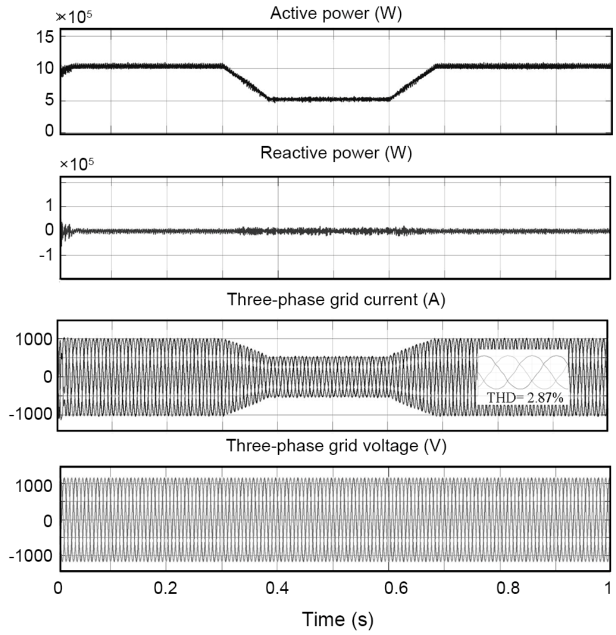

Fig. 14. Simulation results for system operation.

which is decreasing about 500 A by reducing the irradiance level to half. In Fig. 14, the system operation is presented where the active power and three-phase currents are changed by irradiance and reactive power is kept zero to meet unity power factor operation condition. The three-phase currents total harmonic distortion (THD) is 2.87% which is acceptable based of IEC standard.

CONCLUSIONS

In this paper, the novel application of perovskite hybrid materials in PV cells, their advantages and utilization in connection with grid has been proposed. The non-linear specification of perovskite materials and the electrical model and the parameters of these new materials are presented. The appropriate values are calculated for series and shunt resistance of PV cells based on short circuit current and open circuit voltage in selected band-gap energy and reverse saturation current and finally the electrical model of PV cells are provided. Next, the structure of grid-connected PV cells utilizing perovskite materials and utilized MPPT method based on P & O algorithm, the DC/DC converter for boosting the DC output of PV cells, and the DC/AC CSI converter for converting the DC outputs of DC/DC boost converter to AC voltage are presented. The simulation results by MATLAB/SIMULINK illustrated the good detection of maximum power point by MPPT method and appropriate grid current and voltage control even in transient condition.

REFERENCES

[1] International Energy Outlook 2017, https://www.eia.gov/ (accessed: April 2018).

[2] Hou, J. Inganäs, O. Friend, R. H. Gao, F. (2018). Nat. Organic solar cells based on non-fullerene acceptors. Mater, 17, 119.

[3] Cansino, J. M. Pablo-Romero, M. D. P. Rom´an R. and Yniguez, R. (2010). Tax incentives to promote green electricity: an overview of EU-27 countries. Energy Policy, 38(10), 6000–6008.

[4] Jagoda, K. Lonseth, R. Lonseth, A. and Jackman, T. (2011). Development and commercialization of renewable energy technologies in Canada: An innovation system perspective. Journal of Renewable Energy, 36(4), 1266–1271.

[5] Seo, J. Noh, J.H. Seok, S.I. (2016). Rational strategies for ecient perovskite solar cells. Acc. Chem. Res., 49, 562–572.

[6] Green, M.A. Hishikawa, Y. Warta, W. Dunlop, E.D. Levi, D.H. Hohl-Ebinger, J. Ho-Baillie, A.W.Y. (2017). Solar cell eciency tables (version 50). Prog. Photovoltaic Res. Appl., 25 (7), 668–676.

[7] McGehee, M. D. (2009). Nanostructured organic-inorganic hybrid solar cells. MRS Bulletin, 34, 95-100.

[8] Saunders, B.R. Turner, M.L. (2008). Nanoparticle-Polymer Photovoltaic Cells. Adv. Colloid Interface Sci., 138, 1–23.

[9] Kwon, S. Moon, H.C. Lim, K.G. Bae, D.; Jang, S.; Shin, J.; Park, J.; Lee, T.W.; Kim, J.K. (2013). Improvement of power conversion efficiency of P3HT:CdSe hybrid solar cells by enhanced interconnection of CdSe nanorods via decomposable selenourea. J. Mater. Chem. A, 1, 2401–2405.

[10] Gonzalez-Valls I. and Lira-Cantu, M. (2009). Vertically-aligned nanostructures of ZnO for excitonic solar cells: A review. Energy and Environmental Science, 2, 19-34.

[11] Cao, X.; Wang, N.; Kim, X. (2011). Mesoporous CdS spheres for high-performance hybrid solar cells. Electrochim. Acta, 56, 9504–9507.

[12] Noori, K. Giustino, F. (2012). Ideal Energy-Level Alignment at the ZnO/P3HT Photovoltaic Interface. Adv. Funct. Mater., 22, 5089–5095.

[13] Takahashi, Y. Hasegawa, H. Takahashi, Y. Inabe, T. (2013). Hall mobility in tin iodide perovskite CH3NH3SnI3: evidence for a doped semiconductor. J. Solid State Chem., 205, 39–43.

[14] Phillips, L.J. Rashed, A.M. Treharne, R.E. Kay, J. Yates, P. Mitrovic, I.Z. Weerakkody, A. Hall, S. Durose, K. (2016). Maximizing the optical performance of planar $CH_3NH_3PbI_3$ hybrid perovskite heterojunction stacks. Sol. Energy Mater. Sol. Cells, 147, 327–333.

[15] Ponseca Jr., C.S. Savenije, T.J. Abdellah, M. Zheng, K. Yartsev, A. Pascher, T. Harlang, T. Chabera, P. Pullerits, T. Stepanov, A. Wolf, J.P. Sundstrom, V. (2014). Organometal halide perovskite solar cell materials rationalized: ultrafast charge generation, high and microsecond-long balanced mobilities, and slow recombination. J. Am. Chem. Soc., 136, 5189–5192.

[16] Kim, H.D. Ohkita, H. Benten, H. Ito, S. (2016). Photovoltaic performance of perovskite solar cells with diffrent grain sizes. Adv. Mater., 28, 917–922.

[17] Xiao, Z. Dong, Q. Bi, C. Shao, Y. Yuan, Y. Huang, J. (2014). Solvent annealing of perovskite induced crystal growth for photovoltaic-device effciency enhancement. Adv. Mater., 26(37), 6503–6509.

[18] Esram T. and Chapman, P. (2007). Comparison of photovoltaic array maximum power point tracking techniques. IEEE Transactions on Energy Conversion, 22(2), 439–449.

[19] Li, G. Jin, Y. Akram, M. and Chen, X. (2017). Research and current status of the solar photovoltaic water pumping system – A review. Renewable & Sustainable Energy Reviews, 79, 440–458.

[20] Villalva, M. G. Gazoli, J. R. and Filho, E. R. (2009). Comprehensive approach to modelling and simulation of photovoltaic arrays. Power Electronics, IEEE Transactions on, 24, 1198-1208.

[21] Linand, B. R. Dong, J. Y. (2012). New zero-voltage switching DC–DC converter for renewable energy conversion systems. IET Power Electronics. 5(4), 393–400.

[22] Sharma S. and Singh, B. (2012). Control of permanent magnet synchronous generator-based stand-alone wind energy conversion system. IET Power Electronics. 5(8), 1519–1526.

[23] Statista website, World power consumption, https://www.statista.com/statistics/280704/world-power-consumption.

[24] Morales-Caporal, M. Rangel-Magdaleno, J. Peregrina-Barreto, H. and Morales-Caporal, R. (2018). FPGA-in-the-loop simulation of a grid-connected photovoltaic system by using a predictive control. Electrical Engineering. 100(3), 1327– 1337.

[25] Blaabjerg, F. Teodorescu, R. Liserre, M. and Timbus, A. (2006). Overview of control and grid synchronization for distributed power generation systems. IEEE Transactions on Industrial Electronics. 53(5), 1398–1409.

[26] Huang, Y. Wang, J. Peng, F. and Yoo, D. W. Survey of the power conditioning system for PV power generation. 37th IEEE Power Electronics Specialists Conference.

AUTHOR (S) BIOSKETCHES

Payam Alem, Ph.D., Faculty of Engineering, Islamic Azad University Urmia branch, Urmia, Iran, *Email: payamalemi@gmail.com*